Available online at www.derpharmachemica.com

Scholars Research Library

Der Pharma Chemica, 2011, 3 (6):576-590
(http://derpharmachemica.com/archive.html)

ISSN 0975-413X
CODEN (USA): PCHHAX

Weight Loss Measurement and Theoretical Study of New Pyridazine Compound as Corrosion Inhibitor for C38 Steel in Hydrochloric Acid Solution

H. Zarrok [1], H. Oudda [1], A. Zarrouk [2], R. Salghi [3], B. Hammouti [2], M. Bouachrine [4]

[1]Laboratoire des procèdes de séparation, Faculté des Sciences, Université Ibn Tofail BP 242, 14000 Kénitra, Morocco.
[2]LCAE-URAC18, Faculté des Sciences, Université Mohammed I[er] B.P. 717, 60000 Oujda, Morocco.
[3]Ecole Nationale des Sciences Appliquées, Equipe Génie de l'Environnement et de Biotechnologie, B.P 1136, 80000 Agadir, Morocco
[4]UMIM, Faculté Polydisciplinaire de Taza, Université Sidi Mohamed Ben Abdellah, Taza, Morocco.

ABSTRACT

The corrosion inhibition of C38 steel in 1M HCl solution by 5-(2-chlorobenzyl)-2,6-dimethylpyridazin-3-one (CBDP) was studied at temperature range 308–343K by weight loss measurement. The results indicate that the studied compound exhibits good performance as inhibitor for C38 steel corrosion in 1M HCl. The inhibition efficiency increases with decreasing temperature. The outcomes show that inhibition takes place by adsorption of the inhibitor on metal surface. The adsorption of pyridazine takes place according to Langmuir`s adsorption isotherm. Kinetic parameters (activation energy, pre-exponential factor, enthalpy of activation and entropy of activation) as well as thermodynamic parameters (enthalpy of adsorption, entropy of adsorption and Gibbs free energy) were calculated and discussed. Quantum chemical calculations using DFT at the B3LYP/6-31G level of theory was further used to calculate some electronic properties of the molecule in order to ascertain any correlation between the inhibitive effect and molecular structure of 5-(2-chlorobenzyl)-2,6-dimethylpyridazin-3-one.*

Keywords*:* C38 Steel; HCl; Inhibition; Pyridazine; Weight Loss; Langmuir; DFT.

INTRODUCTION

Temperature has a great effect on the rate of metal electrochemical corrosion. In case of corrosion in a neutral solution, the increase of temperature has a favourable effect on the overpotential of oxygen depolarization and the rate of oxygen diffusion, but it leads to a decrease of oxygen solubility. In case of corrosion in an acid medium, the corrosion rate increases with

temperature increase because the hydrogen evolution overpotential decreases. Temperatures effects on acidic corrosion, most often in hydrochloric and sulphuric acids, have been the object of a large number of investigations [1–21]. It is generally assumed that in acid corrosion the inhibitors adsorb on the metal surface, resulting in a structural change of the double layer and reduced rate of the electrochemical partial reaction. The adsorption of inhibitor is influenced by the electronic structure of the inhibiting molecules [22-24] and also by the steric factors, aromaticity, electron density at the donor atoms and also by the presence of functional groups such as C=NH, –N=N–, –CHO, R–OH, C=C, etc.

N-heterocyclic compound receive more and more attention in inhibitory practices to avoid corrosion damage of metals and alloys [11, 25-26]. Adsorption of inhibitors creates a barrier against aggressive ions to reach metallic surface and hence reduce the corrosion rate. Inhibitor molecules then impede by blocking the reactive sites on the surface. Survey of literature shows that pyridazine compounds are efficient inhibitors on the corrosion of metals in acid solution [27-33]. Thus, the inhibitory effect of 5-(2-chlorobenzyl)-2,6-dimethylpyridazin-3-one (CBDP) on C38 steel corrosion in 1M HCl at 308 -343 K was studied by weight loss as well as by quantum chemical studies. The inhibitor adsorption mechanism was studied, and the thermodynamic functions for the dissolution and adsorption processes were calculated and discussed. The choice of this compound was also based on molecular structure considerations, i.e., this is an organic compound with several adsorption centres. The molecular structure of 5-(2-chlorobenzyl)-2,6-dimethylpyridazin-3-one (CBDP) is as shown below:

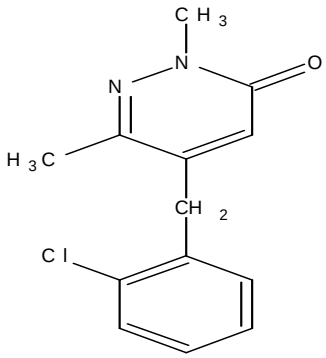

Figure .1 The molecular structure of CBDP.

MATERIALS AND METHODS

2.1. Materials and reagents

C38 Steel strips containing 0.09 wt.% P; 0.38 wt. % Si; 0.01 wt. % Al; 0.05 wt. % Mn; 0.21 wt. % C; 0.05 wt. % S and the remainder iron were used for gravimetric studies. Prior to all measurements, are abraded with a series of emery paper from 180 to 1200 grade. The specimens are washed thoroughly with bidistilled water degreased and dried with acetone. The specimens are washed thoroughly with bidistilled water degreased and dried with acetone. The aggressive solution (1M HCl) was prepared by dilution of Analytical Grade 37 % HCl with double-distilled water.

2.2. Weight loss measurements

Gravimetric measurements are carried out in a double walled glass cell equipped with a thermostated cooling condenser. The solution volume is 50 cm^3. The copper specimens used have a rectangular form (1.6cm × 1.6cm × 0.07cm). The immersion time for the weight loss is 1h.

2.3. Quantum chemical calculations

Complete geometrical optimizations of the investigated molecules are performed using DFT (density functional theory) with the Beck's three parameter exchange functional along with the Lee–Yang–Parr nonlocal correlation functional (B3LYP) [34–36] with 6- 31G* basis set is implemented in Gaussian 03 program package [37]. This approach is shown to yield favorable geometries for a wide variety of systems. This basis set gives good geometry optimizations. The geometry structure was optimized under no constraint. The following quantum chemical parameters were calculated from the obtained optimized structure: the energy of the highest occupied molecular orbital (E_{HOMO}), the energy of the lowest unoccupied molecular orbital (E_{LUMO}), $\Delta E_{gap} = E_{HOMO} - E_{LUMO}$, the dipole moment ($\mu$) and total energy (TE).

RESULTS AND DISCUSSION

3.1. Effect of temperature

Temperature has a great effect on the corrosion phenomenon. Generally the corrosion rate increases with the rise of the temperature. We have studied the temperature influence on the efficiency of CBDP. For this purpose, we made weight-loss measurements in the range of temperature 308–343 K, in the absence and presence of CBDP at different concentrations of this inhibitor. The corresponding data are shown in Table 1.

The corrosion rate (W) was calculated from the following equation:

$$W = \frac{(m_1 - m_2)}{(S.t)} \quad (1)$$

where m_1 is the mass of the specimen before corrosion, m_2 the mass of the specimen after corrosion, S the total area of the specimen, t the corrosion time and W the corrosion rate.

With the calculated corrosion rate, the inhibition efficiency of inhibitor for the corrosion of C38 steel was obtained by using the following equation [38]:

$$IE_w(\%) = (1 - \frac{W_{corr}}{W^{\circ}_{corr}}) \times 100 \quad (2)$$

W_{corr} and W°_{corr} are the corrosion rate of steel samples with and without the inhibitor, respectively.

The degree of surface coverage (Θ) was calculated using equation 3 [38]:

$$\Theta = 1 - \frac{W_{corr}}{W^{\circ}_{corr}} \quad (3)$$

The influence of temperature on the corrosion behaviour of C38 steel/acid added of by 5-(2-chlorobenzyl)-2,6-dimethylpyridazin-3-one (CBDP) at various concentrations is investigated by weight-loss trend in the temperature rang 308-343K during 1h of immerssion. The collected curves in Fig. 2 show the evolution of corrosion rate (CR) with CBDP concentration (C) at different temperatures. Fig. 2 indicates that at a given CBDP concentration the corrosion rate of steel increased with temperature. The values of inhibition efficiency

obtained from the weight loss for different inhibitor concentrations and at various temperatures in 1M HCl are given in Table 1 and Fig. 3. The results show that the inhibition efficiency decreases with increasing temperature indicating that higher temperature dissolution of steel predominates on adsorption of CBDP at the surface. Is clear that inhibition efficiency increased with increase in inhibitor concentration. The maximum value of inhibition efficiency (E_w%) obtained for 10^{-3}M CBDP is 96.1% at 308 K.

Table 1. Gravimetric data of CBDP at different concentrations in 1M HCl at different temperatures

T (K)	Concentration(M)	W(mg/cm^2.h)	E_w (%)	Θ
308	Blank	1.07	-	-
	1×10^{-3}	0.04	96.1	0.961
	5×10^{-4}	0.05	95.2	0.952
	1×10^{-4}	0.06	94.2	0.942
	5×10^{-5}	0.12	88.3	0.883
313	Blank	1.49	-	-
	1×10^{-3}	0.08	94.3	0.943
	5×10^{-4}	0.11	92.8	0.928
	1×10^{-4}	0.14	90.9	0.909
	5×10^{-5}	0.24	83.6	0.836
323	Blank	2.87	-	-
	1×10^{-3}	0.25	91.4	0.914
	5×10^{-4}	0.28	90.1	0.901
	1×10^{-4}	0.36	87.5	0.875
	5×10^{-5}	0.65	77.2	0.772
333	Blank	5.21	-	-
	1×10^{-3}	0.68	86.9	0.869
	5×10^{-4}	0.80	84.7	0.847
	1×10^{-4}	1.06	79.6	0.796
	5×10^{-5}	1.57	69.8	0.698
343	Blank	10.02	-	-
	1×10^{-3}	1.72	82.8	0.828
	5×10^{-4}	1.92	80.8	0.808
	1×10^{-4}	2.69	73.2	0.732
	5×10^{-5}	4.06	59.5	0.595

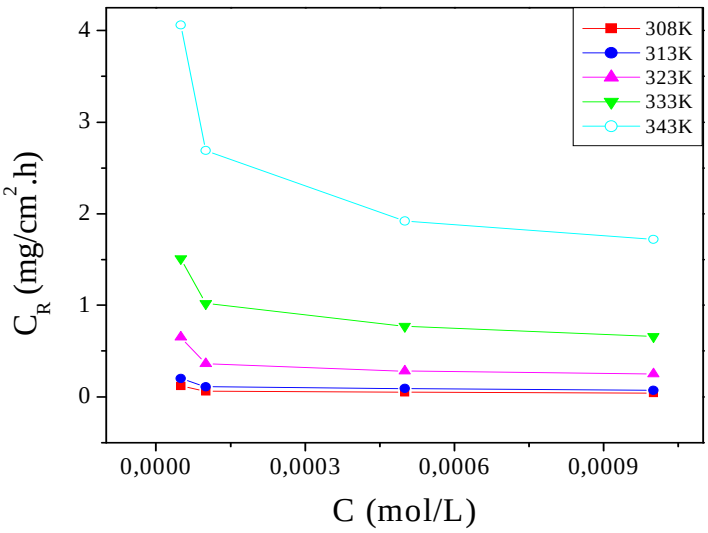

Fig 2. Variation of corrosion rate with the concentrations of CBDP for steel in 1M HCl at different temperatures

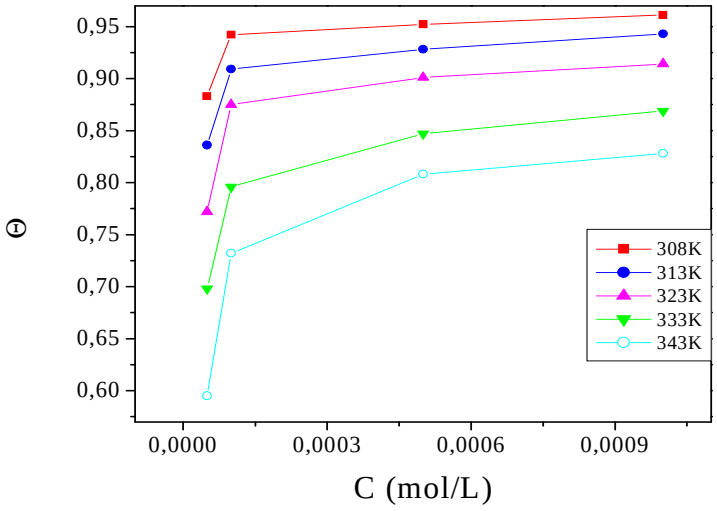

Fig 3. Relationship between inhibition efficiency and concentration of CBDP in 1M HCl.

3.2. Adsorption isotherm and thermodynamic parameters

Adsorption isotherms provide information about the interaction of the adsorbed molecules with the electrode surface [39,40]. The adsorption of an organic adsorbate at metal–solution interface can be presented as a substitution adsorption process between the organic molecules in aqueous solution, (Org (sol)), and the water molecules on metallic surface, (H_2O (ads)) [41]:

$$Org_{(sol)} + nH_2O_{(ads)} \Leftrightarrow Org_{(ads)} + nH_2O_{(sol)}$$

where Org(sol) and Org(ads) are the organic specie dissolved in the aqueous solution and adsorbed onto the metallic surface, respectively, H_2O(ads) is the water molecule adsorbed on the metallic surface and n is the size ratio representing the number of water molecules replaced by one organic adsorbate. In order to obtain the isotherm, the linear relation between degree of surface coverage (Θ) values (Θ = E%/100; Table 1) and inhibitor concentration (C_{inh}) must be found. Attempts were made to fit the Θ values to various isotherms including Langmuir, Temkin, Frumkin and Flory–Huggins. By far the best fit is obtained with the Langmuir isotherm. This model has also been used for other inhibitor systems [42, 43]. According to this isotherm, Θ is related to C_{inh} by:

$$\frac{\Theta}{1-\Theta} = K_{ads}.C_{inh} \qquad (4)$$

Rearranging Eq. 4 gives:

$$\frac{C_{inh}}{\Theta} = \frac{1}{K_{ads}} + C_{inh} \qquad (5)$$

where K_{ads} is the equilibrium constant of the inhibitor adsorption process, C_{inh} is the inhibitor concentration and Θ is the surface coverage that was calculated by Eq. 3. This model for Langmuir's adsorption isotherm has been used extensively in the literatures for various metal/inhibitor/acid solution systems [39, 41, 44-46].

A fitted straight line is obtained for the plot of C_{inh}/Θ versus C_{inh} with slope close to 1 as seen in Fig. 4. The strong correlation ($R^2 > 0.9999$) suggests that the adsorption of inhibitor on the C38

steel surface obeyed this isotherm. This isotherm assumes that the adsorbed molecules occupy only one site and there are no interactions with other adsorbed species [40].

The K_{ads} values can be calculated from the intercept lines on the C_{inh}/Θ-axis. This is related to the standard free energy of adsorption (ΔG°_{ads}) with the following equation 6:

$$\Delta G^{\circ}_{ads} = -RTLn(55.5K_{ads}) \quad (6)$$

where R is the gas constant and T is the absolute temperature. The constant value of 55.5 is the concentration of water in solution in mol/dm^3 [47].

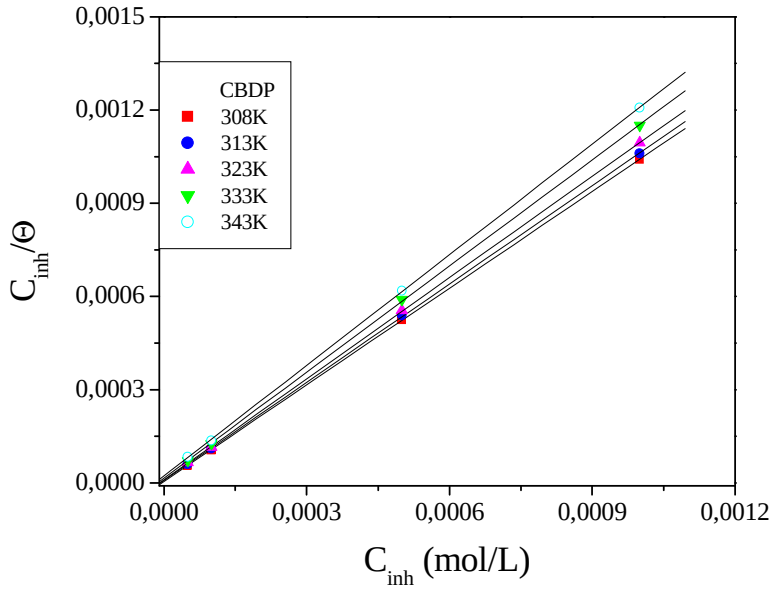

Fig 4. The relationship between C_{inh}/Θ and C of CBDP at various temperatures.

Calculated free energies (ΔG°_{ads}) are given in Table 2; the negative values of ΔG°_{ads} indicate spontaneous adsorption of DMT onto the C38 steel surface [48] and strong interactions between inhibitor molecules and the metal surface [49]. Generally, values of ΔG°_{ads} up to -20 kJ mol^{-1} are consistent with physisorption, while those around -40 kJ mol^{-1} or higher are associated with chemisorption as a result of the sharing or transfer of electrons from organic molecules to the metal surface to form a coordinate [50]. In the present study, the estimated DG°ads values oscillating around -40 kJ.mol^{-1} indicate that the adsorption mechanism of the quinoxaline tested may be a mixed type of physisorption and chemisorption.

Thermodynamically, ΔG°_{ads} is related to the standard enthalpy and entropy of the adsorption process, ΔH°_{ads} and ΔS°_{ads}, respectively, via Eq. (7):

$$\Delta G^{\circ}_{ads} = \Delta H^{\circ}_{ads} - T\Delta S^{\circ}_{ads} \quad (8)$$

and the standard enthalpy of adsorption (ΔH°_{ads}) can be calculated according to the van't Hoff equation [51]:

$$\mathrm{Ln}(K_{ads}) = -\frac{\Delta H^{\circ}_{ads}}{\mathrm{R\,T}} + Constant \quad (9)$$

A plot of Ln K_{ads} versus 1000/T gives a straight line, as shown in Fig. 5. The slope of the straight line is $\Delta H^{\circ}_{ads}/R$. The value of ΔH°_{ads} is given in Table 2. Since the ΔH°_{ads} value is negative, the adsorption of inhibitor molecules onto the C38 steel surface is an exothermic process. In an exothermic process, chemisorption is distinguished from physisorption by considering the absolute value of ΔH°_{ads}; for the chemisorption process, it approaches 100 kJ/mol, while for the physisorption process, it is less than 40 kJ /mol [52,53]. In the present case; the standard adsorption heat -39.299 kJ mol^{-1} shows that a comprehensive adsorption (physical adsorption) might occur [51]. ΔH°_{ads} = -39.299 kJ mol^{-1} found by the Van't Hoff equation, may be also evaluated by the Gibbs–Helmholtz equation, which is defined as follows:

$$\left[\frac{\partial(\Delta G^{\circ}_{ads}/T)}{\partial T}\right]_P = -\frac{\Delta H^{\circ}_{ads}}{T^2} \tag{10}$$

Which can be arranged to give the following equation:

$$\frac{\Delta G^{\circ}_{ads}}{T} = \frac{\Delta H^{\circ}_{ads}}{T} + A \tag{11}$$

The adsorption of inhibitor molecules is accompanied by positive values of ΔS°_{ads}.

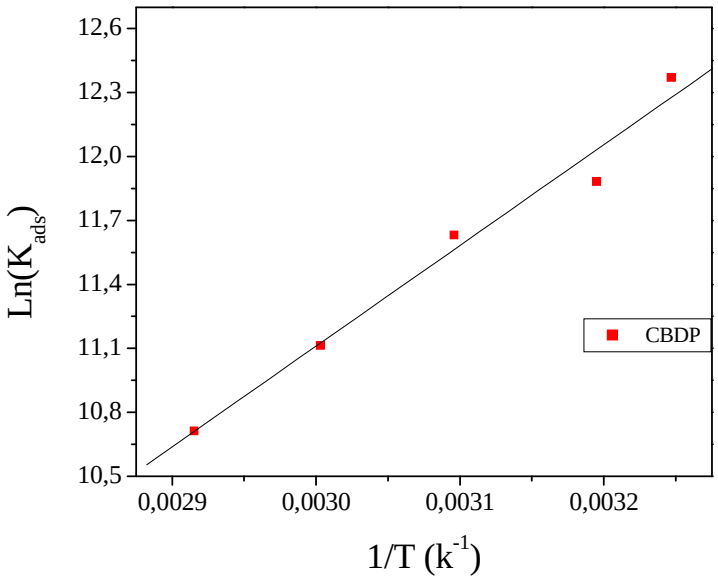

Fig 5. The relationship between Ln(K_{ads}) and 1/T for CBDP.

Fig. 6 shows the variation of $\Delta G^{\circ}_{ads}/T$ with $1/T$ which gives a straight line with a slope that equals ΔH°_{ads}. It can be seen from the figure that $\Delta G^{\circ}_{ads}/T$ decreases with $1/T$ in a linear fashion. The calculated ΔH°_{ads} using the Gibbs–Helmholtz equation is -39.29476 kJ mol^{-1} for CBDP compound, confirming the exothermic behaviour of adsorption on the steel surface, therefore, the values of ΔH°_{ads} obtained by both methods are in good agreement.

Table 2. The thermodynamic parameters of adsorption of CBDP on the steel surface

T (K)	coefficient de régression Linéaire (r)	K_{ads} (L/mol)	ΔG°_{ads} (kJ/mol)	ΔH°_{ads} (kJ/mol)	ΔS°_{ads} (J/mol.K)
308	0.99999	235607.89	-41.960		8.64
313	0.99998	144469.84	-41.369		6.61
323	0.99998	112555.83	-42.020	-39.299	8.42
333	0.99996	66971.16	-41.884		7.76
343	0.99998	44909.51	-42.002		7.88

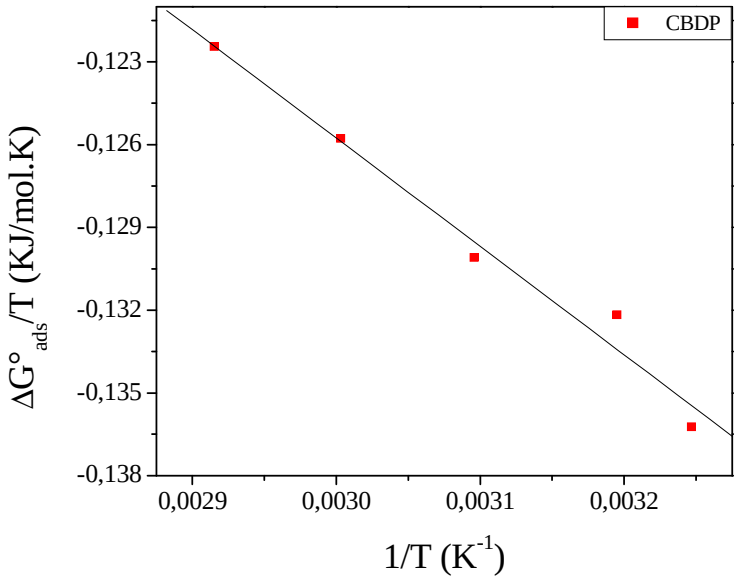

Fig 6. Relationship between ΔG°_{ads}/T and the reverse of absolute temperature.

3.3. Corrosion kinetic parameters

The effect of temperature on the inhibited acid–metal reaction is very complex, because many changes occur on the metal surface such as rapid etching and desorption of inhibitor and the inhibitor itself may undergo decomposition [54]. The change of the corrosion rate with the temperature was studied in 1M HCl, both in absence and presence of 5-(2-chlorobenzyl)-2,6-dimethylpyridazin-3-one (CBDP).

The effect of temperature on the corrosion parameter of C38 steel in 1M HCl was studied at 308, 313, 323, 333 and 343K. The mechanism of inhibition can be deduced by comparing the activation energy in the presence and absence of the inhibitor. The Arrhenius plot and transition state plot were used to determine the activation energy (E_a), activation enthalpy (ΔH°_a), and activation entropy (ΔS°_a) for the corrosion of C38 steel in 1M HCl with and without CBDP. The activation energy can be obtained by the Arrhenius equation and Arrhenius plot:

$$C_R = A\exp\left(\frac{-E_a}{RT}\right) \qquad (12)$$

Where C_R is the corrosion rate, R the gas constant, T the absolute temperature, A the pre-exponential factor. Using the logarithm:

$$LnC_R = \frac{-E_a}{RT} + LnA \quad (13)$$

The graph of Ln (C_R) against 1/T gives a straight line with a slope of ($-E_a/R$). Fig. 7 shows the Arrhenius plot for C38 steel in 1M HCl with the presence and absence of CBDP. Ea was calculated and tabulated in Table 3. The transition state equation was used to calculate the ΔH_a° and ΔS_a°:

$$C_R = \frac{RT}{Nh}\exp\left(\frac{\Delta S_a^\circ}{R}\right)\exp\left(-\frac{\Delta H_a^\circ}{RT}\right) \quad (14)$$

where N is Avogadro's number (6.02×10^{23} mol^{-1}) and h is Plank's constant (6.63×10^{-34} $m^2kg\ s^{-1}$). Eq. (14) looks like an exponential multiplied by a factor that is linear in temperature. However, the activation energy is itself a temperature dependent quantity as follows:

$$E_a = \Delta H_a^\circ - T\Delta S_a^\circ \quad (15)$$

Therefore, when all of the details are worked out one ends up with an expression that again takes the form of an Arrhenius exponential multiplied by a slowly varying function of T. The precise form of the temperature dependence depends upon the reaction, and can be calculated using formulas from statistical mechanics involving the partition functions of the reactants and of the activated complex. Nevertheless, in order to carry simple calculations, Eq. (15) was rearranged to become:

$$Ln(C_R/T) = \left(\frac{-\Delta H_a^\circ}{RT}\right) + \left[Ln\left(\frac{R}{Nh}\right) + \frac{\Delta S_a^\circ}{R}\right] \quad (16)$$

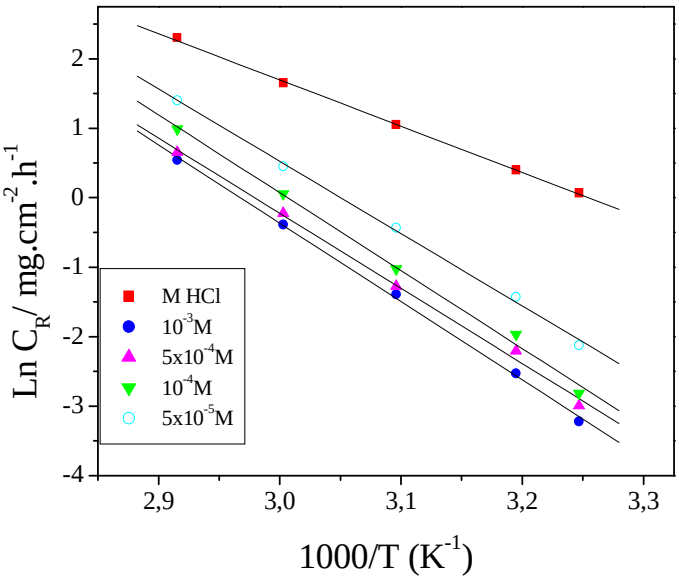

Fig. 7. Arrhenius plots of log C_R vs. 1/T for steel in 1M HCl in the absence and the presence of CBDP at optimum concentration.

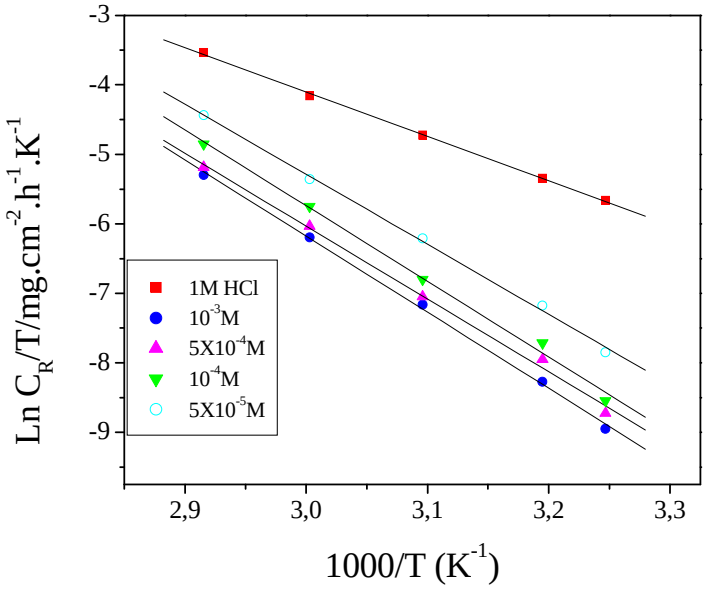

Fig. 8. Arrhenius plots of log C_R/T vs. 1/T for steel in 1M HCl in the absence and the presence of CBDP at optimum concentration

A plot of Ln (C_R/T) against 1/T should give a straight line with a slope of (-ΔH_a°/R) and intercept of [Ln (R/Nh) + (ΔS_a°/R)], as shown in Fig. 8. ΔH_a° and ΔS_a° were calculated and tabulated in Table 3. From Table 3, the activation energy Ea increases in the presence of the inhibitor. Increases in E_a with the presence of CBDP indicate that a physical (electrostatic) adsorption occurred in the first stage. CBDP is an organic nitrogen compound that easily protonates to give a cationic form in acid medium. The E_a value was greater than 20 kJ mol^{-1} in both the presence and absence of the inhibitor, which reveals that the entire process is controlled by the surface reaction [55].

The values of ΔH_a° and E_a are nearly the same and are higher in the presence of the inhibitor. This indicates that the energy barrier of the corrosion reaction increased in the presence of the inhibitor without changing the mechanism of dissolution. The positive values of ΔH_a° for both corrosion processes with and without the inhibitor reveal the endothermic nature of the steel dissolution process and indicate that the dissolution of steel is difficult [11,56].

The large negative value of ΔS_a° for C38 steel in 1M HCl implies that the activated complex is the rate-determining step, rather than the dissociation step. In the presence of the inhibitor, the value of ΔS_a° increases and is generally interpreted as an increase in disorder as the reactants are converted to the activated complexes [11]. The positive values of ΔS_a° reflect the fact that the adsorption process is accompanied by an increase in entropy, which is the driving force for the adsorption of the inhibitor onto the steel surface.

Table 3. The values of activation parameters for C38 steel in 1M HCl in the absence and the presence of different concentrations of CBDP

Conc (M)	A (mg/cm^2.h)	Linear regression coefficient (r)	E_a (kJ/mol)	ΔH_a° (kJ/mol)	ΔS_a° (J/mol.K)	$E_a - \Delta H_a^\circ$ (kJ/mol)
Blank	3.0066×10^{9}	0.99961	55.75	53.05	-72.49	2.7
10^{-3}	3.4177×10^{14}	0.99934	93.76	91.06	24.29	2.7
5×10^{-4}	9.6300×10^{13}	0.99833	89.85	87.15	13.76	2.7
10^{-4}	4.3099×10^{14}	0.99799	93.19	90.49	26.22	2.7
5×10^{-5}	5.9960×10^{13}	0.99903	86.47	83.77	09.82	2.7

We remark that E_a and $\Delta H°_a$ values vary in the same way with the inhibitor concentration (Fig. 9 and Table 3). This result permits to verify the known thermodynamic relation between E_a and $\Delta H°_a$ as shown [57]:

$$E_a - \Delta H_a^\circ = RT \quad (17)$$

The calculate values are too close to RT is 2.7 kJ/mol. This result shows the inhibitor acted equally on E_a and ΔH_a°.

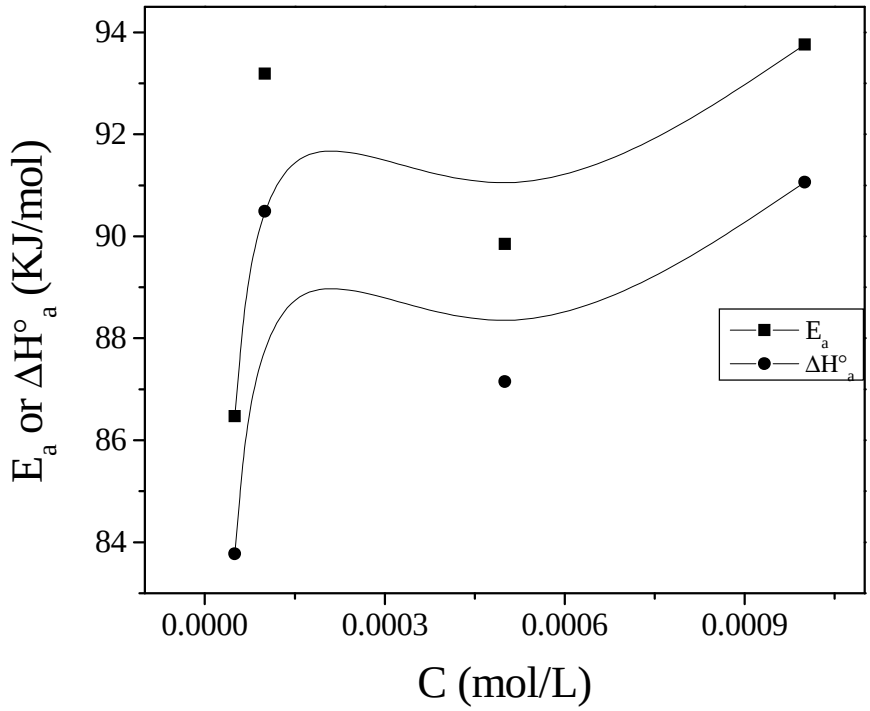

Fig 9. The relationship between E_a and ΔH_a° with concentration of CBDP.

3.4. Quantum chemical calculations

Quantum chemical methods and molecular modeling techniques enable the definition of a large number of molecular quantities characterizing the reactivity, shape, and binding properties of a complete molecule as well as of molecular fragments and substituents. The geometry of the inhibitor as well as the nature of its frontier molecular orbitals, namely, the HOMO and LUMO is involved in the activity properties of the inhibitors. Therefore, in this study, quantum chemical

calculations were performed to investigate the relationship between molecular structure of this compound and their inhibition effect. The optimized molecular structure and the frontier molecule orbital density distribution of the studied molecule are shown in Fig. 10, and the calculated quantum chemical parameters E_{HOMO}, E_{LUMO}, ΔE (E_{LUMO} - E_{HOMO}), dipole moment (μ), number of transferred electrons (ΔN), and total energy (TE) are given in Table 4.

Frontier orbital theory is useful in predicting adsorption centers of the inhibitor molecules responsible for the interaction with surface metal atoms [58, 59]. Terms involving the frontier MO could provide dominative contribution, because of the inverse dependence of stabilization energy on orbital energy difference [58]. It has been reported in the literature that the higher the HOMO energy of the inhibitor, the greater the trend of offering electrons to unoccupied d orbital of the metal, and the higher the corrosion inhibition efficiency. In addition, the lower the LUMO energy, the easier the acceptance of electrons from metal surface, as the LUMO–HOMO energy gap decreased and the efficiency of inhibitor improved [60]. The dipole moment (μ) of CBDP is 3.7649 Debye (12.56×10^{-30} C.m), which is higher than that of H_2O ($\mu = 6.20\times10^{-30}$ C.m). The high value of dipole moment probably increases the adsorption between chemical compound and metal surface [61]. Accordingly, the adsorption of CBDP molecules from the aqueous solution can be regarded as a quasi-substitution process between the CBDP compound in the aqueous phase [CBDP(sol)] and water molecules at the electrode surface [H_2O(ads)].

Analysis of Fig. 10 shows that the distribution of two enrgies HOMO and LUMO localized in the atoms of pyridazine cycle, consequently this is the favourite sites for interaction with the metal surface. The total energy of the CBDP is equal to -1148.129374 Kcal/mol. This result indicated that CBDP is favourably adsorbed through the active centers of adsorption.

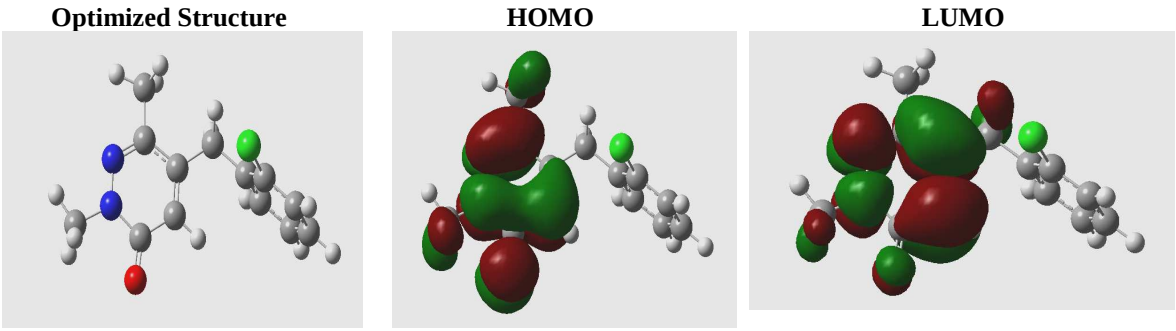

Fig. 10. Optimized structure and frontier orbital distribution of the test molecule.

The number of transferred electrons (ΔN) was also calculated according to Eq. (18) [62, 63]

$$\Delta N = \frac{\chi_{Fe} - \chi_{inh}}{2(\eta_{Fe} + \eta_{inh})} \qquad (18)$$

where χ_{Fe} and χ_{inh} denote the absolute electronegativity of iron and the inhibitor molecule, respectively; η_{Fe} and η_{inh} denote the absolute hardness of iron and the inhibitor molecule, respectively. These quantities are related to electron affinity (A) and ionization potential (I)

$$\chi = \frac{I + A}{2}, \eta = \frac{I - A}{2}$$

I and A are related in turn to E_{HOMO} and E_{LUMO}

$I = -E_{HOMO}$ and $A = -E_{LUMO}$

Values of χ and η were calculated by using the values of I and A obtained from quantum chemical calculation. The theoretical values of χ_{Fe} and η_{Fe} are 7 and 0 eV/mol, respectively [62]. The fraction of electrons transferred from inhibitor to the iron molecule (ΔN) was calculated. According to other reports [62, 63], value of ΔN showed inhibition effect resulted from electrons donation. In this study, the CBDP was the donators of electrons while the C38 steel surface was the acceptor. The CBDP was bound to the C38 steel surface, and thus formed inhibition adsorption layer against corrosion.

Table 3. Calculated quantum chemical parameters of studied inhibitor

Compound	TE (Kcal/mol)	E_{HOMO} (eV)	E_{LUMO} (eV)	ΔE_{gap} (eV)	μ (Debye)	ΔN (eV)
CBDP	-1148.129374	- 6.0521	- 1.2934	4.758	3.7649	-2.24279

CONCLUSION

The following conclusions may be drawn from the study:

- Results obtained show that pyridazine tested is an efficient inhibitor.
- Inhibition efficiency increases with the increase of concentration to attain 96.1% at 10^{-3}M.
- The inhibition efficiency decreased with increasing temperature as a result of the higher dissolution of steel at higher temperature. The addition of CBDP leads to an increase of the activation energy of the corrosion process. The adsorption equilibrium constant (K_{ads}) decreased with increasing temperature. The negative value of ΔG°_{ads} is a sign of spontaneous adsorption on the metal surface.
- Kinetic and adsorption parameters were evaluated and discussed.
- Quantum chemical parameters such as E_{HOMO}, E_{LUMO}, ΔE (E_{LUMO} - E_{HOMO}), dipole moment (μ), number of transferred electrons (ΔN), and total energy (TE) were found to give good correlation with experimentally determined inhibition efficiency.

REFERENCES

[1] N.P. Zhuk, Course on Corrosion and Metal Protection, Metallurgy, Moscow, **1976**.
[2] G. Perboni and G. Rocchini, Proceedings of the 10th ICMC, Madras, India, **1988**, p. 2763.
[3] I.H. Omar, G. Trabanelli and F. Zucchi, Proceedings of the 10th ICMC, Madras, India, **1988**, p. 2723.
[4] R.P. Mathur and T. Vasudevan, *Corros.*, 38 (**1982**) 171.
[5] F. Zucchi and G. Trabanelli, Proceedings of the 7th European Symposium on Corrosion Inhibitors, Ferrara, **1990**, p. 339.
[6] E. McCafferty and N. Hackerman, *J. Electrochem. Soc*., 119 (**1972**) 999.
[7] R. Hariharaputhran, A. Subramanian, A.A. Antony, P.M. Sankar, A. Gopalan, T. Vasudevan and I.S Vencatakrishna, *Br. Corros. J.*, 33 (**1998**) 214.
[8] E. S. Ivanov, Inhibitors for Metal Corrosion in Acid Media, Metallurgy, Moscow, **1986**.
[9] Z. A. Foroulis, Proceedings of the 6th European Symposium on Corrosion Inhibitors, Ferrara, **1985**, p. 48.
[10] Q.J. Slaiman and H.M. Al-Saaty, Proceedings of the 7th European Symposium on Corrosion Inhibitors, Ferrara, **1990**, p. 149.

[11] I. El Ouali, B. Hammouti, A Aouniti, Y. Ramli, M. Azougagh, E.M. Essassi, M. Bouachrine, J. Mater. Envir. Sci. 1 N° 1 (**2010**) 1-8.
[12] M. Elayyachy, B. Hammouti, A. El Idrissi and A. Aouniti, *Portugaliae Electrochimica Acta* **2011**, 29(1), 57-68.
[13] M. Benabdellah, A. Tounsi, K.F. Khaled, B. Hammouti, *Arabian Journal of Chemistry* (**2011**) 4, 17–24.
[14] M. Bouklah, B. Hammouti, M. Lagrene´e, F. Bentiss, *Corrosion Science* 48 (**2006**) 2831–2842.
[15] M. Bouklah, B. Hammouti, *Portugaliae Electrochimica Acta* 24 (**2006**) 457-468.
[16] L. Herrag, B. El Bali, M. Lachkar and B. Hammouti, *Oriental Journal of Chemistry* Vol. 25(2), 265-272 (**2009**).
[17] Ehteram A. Noor, *Int. J. Electrochem. Sci.*, 2 (**2007**) 996 – 1017.
[18] Eno E. Ebenso, Ime B. Obot, *Int. J. Electrochem. Sci*., 5 (**2010**) 2012 – 2035.
[19] 19. N.O. Obi-Egbedi, K.E. Essien, I.B. Obot, E.E. Ebenso, *Int. J. Electrochem. Sci*., 6 (**2011**) 913 – 930.
[20] M. Benabdellah, K. Tebbji, B. Hammouti, R. Touzani, A. Aouniti, A. Dafali, S. El Kadiri, *Phys. Chem. News* 43 (**2008**) 115-120.
[21] N. O. Obi-Egbedi, I. B. Obot, *Corrosion Science* 53 (**2011**) 263-275.
[22] S. S. Abd El Rehim, M. A. M. Ibrahim, K. F. Khalid, *J. Appl. Electrochem*., 29 (**1999**) 593.
[23] I. Zaafarany, M. Abdallah, *Int. J. Electrochem. Sci*., 5 (**2010**) 18.
[24] K. Nageh Allam, *Applied Surface Science*., 253 (**2007**) 4570.
[25] A. Zarrouk, A. Dafali, B. Hammouti, H. Zarrok, S. Boukhris, M. Zertoubi, *Int. J. Electrochem. Sci.*, 5 (**2010**) 46.
[26] M. Benabdellah, R. Touzani, A. Aouniti, A. Dafali, S. Elkadiri, B. Hammouti, M. Benkaddour, *Phys. Chem. News*, 37 (**2007**) 63.
[27] M. Bouklah, N. Benchat, B. Hammouti, A. Aouniti, S. Kertit, *Materials Letters*., 60 (**2006**) 1901.
[28] A. Chetouani, B. Hammouti, A. Aouniti, N. Benchat, T. Benhadda, *Prog. Org. Coat*., 45 (**2002**) 373.
[29] Deana Wahyuningrum, Sadijah Achmad, Yana Maolana Syah, Buchari, Bunbun Bundjali, Bambang Ariwahjoedi, *Int. J. Electrochem. Sci*., 3 (**2008**) 154.
[30] M. Bouklah, N. Benchat, A. Aouniti, B. Hammouti, M. Benkaddour, M. Lagrenée, H. Vezin, F. Bentiss, *Org. Coat*., 51 (**2004**) 118.
[31] A. Zarrouk, A. Chelfi, A. Dafali, B. Hammouti, S. S. Al-Deyab, I. Warad, N. Benchat, M. Zertoubi, *Int. J. Electrochem. Sci*., 5 (**2010**) 696.
[32] A. Zarrouk, I. Warad, B. Hammouti, A Dafali, S.S. Al-Deyab, N. Benchat, *Int. J. Electrochem. Sci.*, 5 (**2010**) 1516 – 1526.
[33] H. Zarrok, R. Saddik, H. Oudda, B. Hammouti, A. El Midaoui, A. Zarrouk, N. Benchat, M. Ebn Touhami, *Der Pharma Chemica*, 3 (**2011**) 272-282.
[34] A. D. Becke, *J. Chem. Phys*., 96 (**1992**) 9489.
[35] A. D. Becke, *J. Chem. Phys*., 98 (**1993**) 1372.
[36] C. Lee, W. Yang, R.G. Parr, *Phys. ReV*. B., 37 (**1988**) 785.
[37] Gaussian 03, Revision B.01, M. J. Frisch, et al., Gaussian, Inc., Pittsburgh, PA, **2003**.
[38] S. R. Lodha, *Pharmaceutical Reviews*. 6 (**2008**) 1.
[39] Ehteram A. Noor, Aisha H. Al-Moubaraki, *Materials Chemistry and Physics* 110 (**2008**) 145–154.
[40] Guls_en Avci, Corrosion inhibition of indole-3-acetic acid on mild steel in 0.5 M HCl, Colloids and Surfaces A: Physicochemical and Engineering Aspects 317 (**2008**) 730–736.
[41] Esmaeel Naderi, A.H. Jafari, M. Ehteshamzadeh, M.G. Hosseini, *Materials Chemistry and Physics* 115 (**2009**) 852–858.

[42] M. Kissi, M. Bouklah, B. Hammouti, M. Benkaddour, *Appl. Surf. Sci*. 252 (**2006**) 4190.
[43] E. Machnikova, K.H. Whitmire, N. Hackerman, *Electrochim. Acta* 53 (**2008**) 6024.
[44] R. Solmaz, G. Kardas_, M. Culha, B. Yazici, M. Erbil, *Electrochimica Acta* 53 (**2008**) 5941–5952.
[45] E. Machnikova, Kenton H. Whitmire, N. Hackerman, *Electrochimica Acta* 53 (**2008**) 6024–6032.
[46] F. Xu, J. Duan, S. Zhang, B. Hou, *Materials Letters* 62 (**2008**) 4072–4074.
[47] O. Olivares, N. V. Likhanova, B. Gomez, J. Navarrete, M. E. Llanos-Serrano, E. Arce, J. M. Hallen, *Appl. Surf. Sci.* 252 (**2006**) 2894.
[48] L. Tang, X. Li, L. Lin, G. Mu, G. Liu, *Mater. Chem. Phys*. 97 (**2006**) 301–307.
[49] ZOR Sibel, Pinar Dogan, Birgul Yazici, *Corros. Rev.* 23 (**2005**) 217–233.
[50] G. Moretti, F. Guidi, G. Grion, *Corros. Sci*. 46 (**2004**) 387–403.
[51] L. B. Tang, G. N. Mu, G. H. Liu, *Corr. Sci*., 45 **(2003)** 2251.
[52] M. Benabdellah, R. Touzani, A. Dafali, M. Hammouti, S. El Kadiri, *Mater. Lett*. 61 (**2007**) 1197–1207.
[53] E. A. Noor, A. H. Al-Moubaraki, *Mater. Chem. Phys*. 110 (**2008**) 145–154.
[54] F. Bentiss, M. Lebrini, M. Lagrenee, *Corrosion Science* 47 (**2005**) 2915–2931.
[55] L. Herrag, B. Hammouti, S. Elkadiri, A. Aouniti, C. Jama, H. Vezin, F. Bentiss, *Corros. Sci*. 52 (**2010**) 3042–3051.
[56] M. Behpour, S.M. Ghoreishi, N. Soltani, M. Salavati-Niasari, M. Hamadanian, A. Gandomi, *Corros. Sci*. 50 (**2008**) 2172–2181.
[57] M. Stern, A. L. Geary, *J. Electrochem. Soc*. 104 (**1957**) 56.
[58] J. Fang, J. Li, *J. Mol. Struct*. (THEOCHEM) 593 (**2002**) 179.
[59] G. Bereket, E. Hur, C. Ogˇretir, *J. Mol. Struct*. (THEOCHEM) 578 (**2002**) 79.
[60] K.F. Khaled, *Appl. Surf. Sci*. 255 (**2008**) 1811.
[61] K. Ramji, D.R. Cairns, S. Rajeswari, *Appl. Surf. Sci.* 254 (**2008**) 4483.
[62] H. Ju, Z. Kai, Y. Li, *Corros. Sci*. 50 (**2008**) 865.
[63] I. Lukovits, E. Kalman, F. Zucchi, *Corrosion* (NACE) 57 (**2001**) 3.